ACCOUNTS
of chemical research

Accurate Simulation of Optical Properties in Dyes

DENIS JACQUEMIN,*,† ERIC A. PERPETE,† ILARIA CIOFINI,‡ AND CARLO ADAMO*,‡

†*Laboratoire de Chimie Théorique Appliquée, Facultés Universitaires Notre-Dame de la Paix, rue de Bruxelles 61, B-5000 Namur, Belgium,* ‡*Laboratoire d'Électrochimie et Chimie Analytique, CNRS UMR-7575, Ecole Nationale Supérieure de Chimie de Paris, 11 rue P. et M. Curie, F-75231 Paris Cedex 05, France*

RECEIVED ON JULY 20, 2008

CONSPECTUS

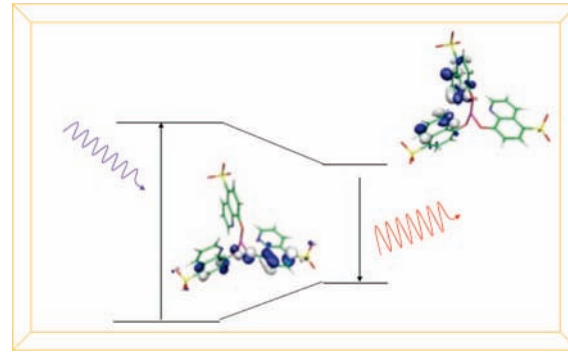

Since Antiquity, humans have produced and commercialized dyes. To this day, extraction of natural dyes often requires lengthy and costly procedures. In the 19th century, global markets and new industrial products drove a significant effort to synthesize artificial dyes, characterized by low production costs, huge quantities, and new optical properties (colors). Dyes that encompass classes of molecules absorbing in the UV−visible part of the electromagnetic spectrum now have a wider range of applications, including coloring (textiles, food, paintings), energy production (photovoltaic cells, OLEDs), or pharmaceuticals (diagnostics, drugs). Parallel to the growth in dye applications, researchers have increased their efforts to design and synthesize new dyes to customize absorption and emission properties. In particular, dyes containing one or more metallic centers allow for the construction of fairly sophisticated systems capable of selectively reacting to light of a given wavelength and behaving as molecular devices (photochemical molecular devices, PMDs).

Theoretical tools able to predict and interpret the excited-state properties of organic and inorganic dyes allow for an efficient screening of photochemical centers. In this Account, we report recent developments defining a quantitative ab initio protocol (based on time-dependent density functional theory) for modeling dye spectral properties. In particular, we discuss the importance of several parameters, such as the methods used for electronic structure calculations, solvent effects, and statistical treatments. In addition, we illustrate the performance of such simulation tools through case studies. We also comment on current weak points of these methods and ways to improve them.

1. Introduction

Since Antiquity, dyes have been intensively produced and commercialized by men. Archaeological evidences found for Tyrian purple (TP, an indigo derivative) date its use back to 1900 BC, while Pliny the Elder in his *Naturalis Historia* gives a detailed description of the process of TP extraction from *Murex* sea snails. For many natural dyes still, extraction often required lengthy and costly procedures. The development of a global market and new industrial products induced a significant effort to synthesize artificial dyes, characterized by low production costs, huge quantities, and new optical properties (colors). While in 1914 96% of the indigo world production was of artificial origin, the first synthetic dye (that is, human-designed), mauveine, appeared as early as 1856. Nowadays, dyes encompassing classes of molecules absorbing in the UV−visible part of the electromagnetic spectrum have a wider range of

Published on the Web 12/29/2008 www.pubs.acs.org/acr
10.1021/ar800163d CCC: $71.50

applications, including coloring (e.g., textile, food, painting), energy production (e.g., photovoltaic, OLED), or medical purposes (e.g., diagnosis, drugs).[1]

Parallel to the growing number of applications, a great effort has been spent in the design and synthesis of new dyes, in order to customize absorption and emission properties (wavelengths and intensities). In particular, inorganic dyes containing metallic center(s) have recently become fashionable systems since developments in design, synthesis, and characterization of supramolecular architectures[2,3] nowadays allow for the construction of fairly sophisticated systems capable of selectively reacting to a given external input (light) and behaving as devices at the molecular level (photochemical molecular devices, PMDs).[4]

In this context, theoretical simulations can act at two different levels: the interpretation and the prediction of optical properties. Indeed, a great precision (of the order of half a nanometer) in the simulation of such properties is required for both technological and coloring applications. In conjunction, an accurate prediction often means a rapid screening of photocenters and consequently allows the establishment of structure−property relationships that help in the design of new compounds.

In the present Account, we report recent developments setting up a quantitative ab initio protocol for modeling dye spectral properties. We first discuss the various parameters, such as the method used for the electronic calculations or for solvation effects, as well as the possible statistical treatments, that enter our global scheme. Then some case studies are detailed with the aim of giving a flavor of the actual performance of our protocol. Besides the large part that is devoted to the calculation of the absorption spectra, we briefly comment on the emission (here fluorescence) spectra and give practical examples. Some remarks concerning the current drawbacks of the methods, as well as possible improvements, are finally listed.

2. The Computational Approach

Electronic methods constitute undoubtedly the main ingredient for a reliable protocol to evaluate optical properties of dyes, and therefore, the choice of the related computational parameters must be carefully performed to avoid the introduction of significant bias. Environmental effects must be introduced in simulations if a quantitative agreement between theory and experiments is targeted. All these aspects, combined with a statistic treatment, allow definition of an error bar on the calculation results. As a consequence, the protocol is able not only to interpret optical properties of experimentally characterized systems but also to predict the behavior of new chromophores.

2.1. Electronic Aspects: DFT, TD-DFT, and Atomic Basis Set. Nowadays, it is well established that the Kohn−Sham approach to density functional theory (DFT) can provide an accurate description of a large number physicochemical properties for the ground state.[5] Furthermore, the current performance/accuracy ratio tends to exceed that of more sophisticated post-Hatree−Fock (post-HF) approaches.

In contrast, the situation for excited electronic states is often more involved. In fact, from one side, fast and cheap purposely tailored semiempirical approaches lack consistency when applied to families of molecules not included in the original training sets. From the other side, more reliable theoretical tools such as post-HF methods are, in most cases, too expensive to afford the study of the large solvated systems of chemical and industrial interest.

The development of the time-dependent density functional approaches (TD-DFT),[6] including the recent implementation of their analytical energy gradients,[7,8] allows for the extension of the ground-state DFT efficiency to excited states. However, as for the ground state, the choice of the exchange−correlation functional form, which is the only approximated term in DFT, plays a key role in reaching chemically sound results. Concerning the UV−vis absorption spectra simulation, the local density approximation (LDA) tends to strongly underestimate valence excitation energies of most organic molecules, whereas better performances are obtained with the generalized gradient approximations (GGAs) or with meta-GGA approaches. The most accurate values are usually predicted by hybrid functionals, which explicitly include a fraction of HF exchange. Aiming for a classification, three different families of hybrid functionals can be defined. The first is composed by global hybrids (GHs), in which the percentage of HF exchange is constant at each point in space. To the second family belong the local hybrids (LHs), characterized by a mixing of HF exchange that depends on the spatial electronic coordinate. Finally, range-separated hybrids (RSHs) use a growing fraction of exact exchange as the interelectronic distance increases, giving a long-range correction (LC) to the original DFT scheme. The B3LYP,[9] *Lh*-BLYP,[10] and LC-PBE[11] functionals are respective prototypes of these three classes.

Here, we mainly focus on the most widespread GHs and, in particular, on B3LYP and PBE0.[12] On the one hand, B3LYP has de facto become a standard for DFT calculations. On the other hand, we have shown that the PBE0 functional, containing 25% HF exchange, generally outperforms other global hybrids in the computation of UV−vis spectra, so it can be

considered as a reference functional for this property (see below). Furthermore PBE0 can be used as a "multipurpose" approach since it yields appropriate simulations for many other chemicophysical properties, thus providing a theoretically consistent description of both ground- and excited-state properties.[12,13]

Finally, it is worth mentioning that the choice of the basis set also plays a relevant role, even though TD-DFT appears to be less basis set dependent than post-HF methods. In our experience, a medium size basis set like valence double- or triple-ζ basis already gives converged results for valence transitions when both polarization and diffuse functions are added. In particular, the Pople's 6-311+G(2d,p) provides converged transition energies of low-lying states for the majority of investigated dyes, while the compact 6-31+G(d) basis represents a valuable compromise between accuracy and computational speed. Concerning metal atoms, the basis set effect seems even less pronounced so that standard pseudopotentials, such as those developed by Hay and Wadt, are often found to be well suited. However, we have shown that when higher energy states (e.g., Rydberg) are sought, larger basis sets, including very diffuse functions, are mandatory.[14]

2.2. Modeling Solvent Effects. Electronic transitions energies are affected by the surroundings, inclusion of which rapidly appears to be crucial for their quantitative simulations, especially if polar groups are directly exposed to the solvent. However, calculations performed on isolated molecules can often provide qualitative trends. The magnitude of the solvent-induced shift strongly depends not only on the nature of the solvent (polar or not, protic or not) but also on the nature of the excitation under investigation. In organic molecules, n$-\pi^*$ transitions are more affected than $\pi-\pi^*$ transitions because the variation of the electronic distribution is larger in the former case; it is also enhanced in protic solvents, which obviously tend to interact with the lone pair. Several reliable approaches have been developed for solvent modeling in ab initio simulations. Accurate simulation of bulk effects for both nonpolar and polar solvents can be obtained by polarizable continuum models (PCMs),[15] possibly including nonequilibrium effects in TD-DFT calculations.[16] More problematic is the simulation of protic solvents, where specific H-bonding interactions can modify the electronic structure of the solute. In that case, the best compromise is represented by mixed models, where all molecules involved in the interactions (e.g., the first solvation shell) are explicitly considered in the electronic calculations and then embedded in a PCM to simulate the bulk effect. A precise determination of the orientation of the solvent molecules has usually a negligible effect with respect to their inclusion and can be simply determined by standard structure minimization procedures without going for more expensive dynamic approaches.

2.3. Defining an Error Bar: The Role of a Statistical Treatment. To improve the agreement between theory and experiment, the results of several approaches can be advantageously combined. To obtain the most efficient combination, multiple linear regression (MLR), based on the numerical technique of least-squares fitting and analyzing the relationship between one dependent variable (experimental value) and p independent variables (theoretical values), is a method of choice. To test the significance of a regression curve, the total sum of squares (TSS) is split into two components, the model sum of squares (MSS) and the residual sum of squares (RSS)

$$\mathrm{TSS} = \mathrm{MSS} + \mathrm{RSS} \tag{1}$$

$$\sum_{i=1}^{n} [y_i - \bar{y}]^2 = \sum_{i=1}^{n} [y_i(x_i) - \bar{y}]^2 + \sum_{i=1}^{n} [y_i - y_i(x_i)]^2 \tag{2}$$

with n being the number of points (here dyes) considered, y_i the experimental quantities, $y(x_i)$ the regression data, and $\bar{y}$ the average values (here transition energies or wavelengths). If the fitted curve passes through all the original data points, MSS is equal to TSS, and RSS is zero. This can be the case if there are numerous descriptors (p) and only a few data points (n). Therefore, one uses an adjusted correlation coefficient (R_{adj}^2):

$$R_{\mathrm{adj}}^2 = 1 - \frac{n-1}{n-p-1}\left(1 - \frac{\mathrm{RSS}}{\mathrm{MSS}}\right) \tag{3}$$

Reliability limits for the regression parameters, measuring the adequacy of each independent variable in the model are also determined, allowing to step-by-step removoval of the less significant independent variables. MLR provides not only the usual mean absolute error (MAE) but also a standard deviation, d_{R}:

$$d_{\mathrm{R}} = \sqrt{\frac{\mathrm{RSS}}{n-p-1}} \tag{4}$$

which is useful for the prediction of properties of compounds not included in the training set.

3. Cases Studies

In the past few years, we have studied a large number of dyes, including both organic and inorganic compounds. Here, we will report only representative examples of transition types both in organic molecules and in coordination complexes.

3.1. Absorption of Organic Molecules. 9,10-Anthraquinone (AQ) derivatives (Figure 1) represent about 1/3 of

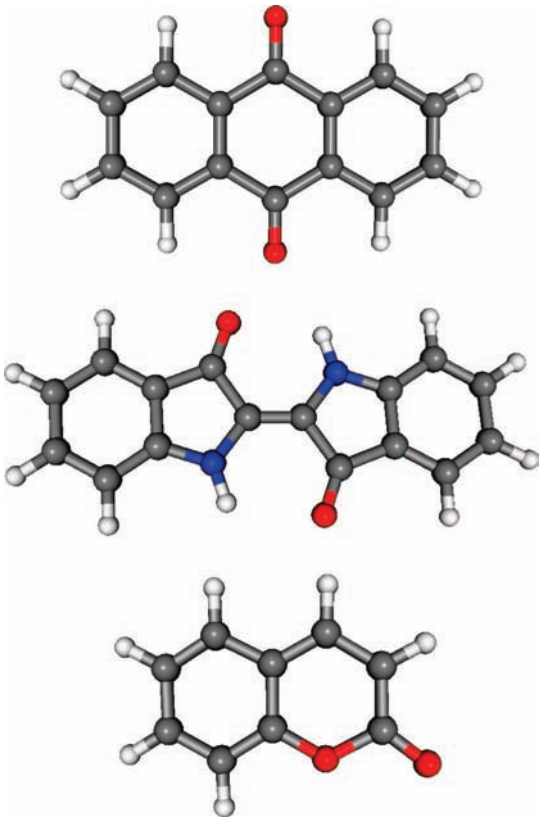

FIGURE 1. Sketches of the basic organic dyes investigated. From top to bottom: 9,10-anthraquinone; prototypical indigo; prototypical coumarin.

today's world organic dye production. This success originates in the stability, easy synthesis, and versatile applications of AQs.[1] In a series of works,[17−20] we have shown that combining the results obtained with the B3LYP and PBE0 functionals provides very accurate estimates of the λ_{max}. In general, the B3LYP hybrid tends to be more efficient for long-wavelength AQ derivatives that typically display a strong intramolecular hydrogen bond between the carbonyl and the side amino groups, whereas PBE0 works best for the hydroxy-AQs.[17,18] It was also shown that extending the basis set further than 6-31G(d,p) is useless;[18,21] that is, in this peculiar case, diffuse functions do not provide more accurate (before fitting) or consistent (after fitting) transition energies. Using all the data from refs 18−20, we designed a set of 189 AQ derivatives solvated in various media (CH_2Cl_2, MeOH, and EtOH), including a large panel of standard substitutions as well as complex laser dyes. Prior to fitting, the mean absolute deviations (MAEs) are 0.10 eV for both functionals. It is worth pointing out that such an accuracy exceeds the generally accepted error for TD-DFT calculations (gas-phase = 0.3 eV) and, of course, that obtained with a CIS approach, 0.58 eV.[21] Optimizing the MLR coefficients for this 189-AQ set leads to

$$\lambda_{max}^{exp} = -33.48 - 0.6845\lambda_{max}^{B3LYP} + 1.80535\lambda_{max}^{PBE0} \quad (5)$$

which provides average deviations limited to 0.08 eV, that is, 20% better than the raw B3LYP or PBE0 values. From the comparison of simulated and experimental wavelengths of Figure 2, it is indeed obvious that there is an excellent agreement between theory and experiment. Indeed, less than 15% of the cases present unacceptable deviations (>0.15 eV). This means that the absorption spectra of substituted AQ can be accurately foreseen at an affordable computational cost.

Another striking example of the efficiency of TD-DFT for simulating the absorption spectra of organic dyes is provided by the indigoid derivatives.[22−24] From a methodological point of view, indigoids are the typical systems for which a second set of polarization functions is required to reach λ_{max} convergence. Studies have also clearly demonstrated that B3LYP is to be favored over PBE0 only when at least one internal NH−O═C hydrogen bond is formed.[24] Using the PCM-TD-DFT/6-311+G(2d,p)//PCM-DFT/6-311G(d,p) approach, we have determined a λ_{max} of 304 indigoid derivatives, including compounds with several heteroatoms (indigo, thioindigo, selenoindigo), various substitutions on the outer phenyl rings (Tyrian purple, nitro derivatives), differently linked (indirubin, isoindigo), or conformers (cis/trans), and solvated in a wide panel of solvents. For this large set, which covers the full width of the visible part of the electromagnetic spectrum,[22−24] we obtain a MAE limited to 0.04 eV, which is basically 1 order of magnitude smaller than the expected 0.3 eV average deviation, although absolutely no statistical correction was performed. Because similar accuracy levels have been found for

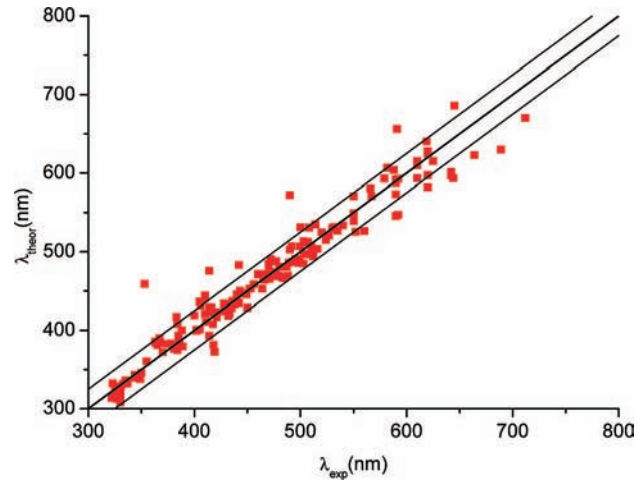

FIGURE 2. Comparison between experimental and theoretical absorption wavelengths for 189 AQ dyes. The theoretical values are obtained using the MLR definition on the basis of PCM-TD-(B3LYP/PBE0)/6-31G(d,p)//B3LYP/6-31G(d,p) raw data. The central line indicates a perfect theory/experiment match, whereas the two side lines are boundaries for ±25 nm deviation.

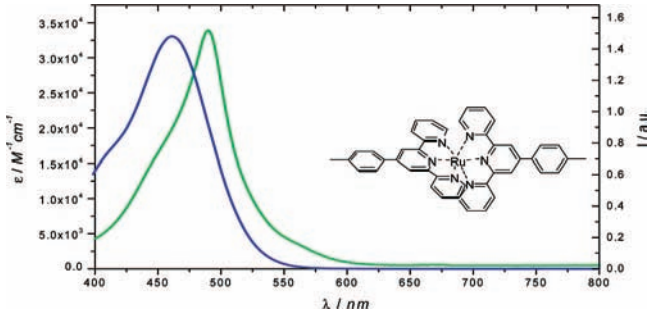

FIGURE 3. Calculated (blue, full width at half-maximum, fwhm = 0.1 eV) and experimental (green) absorption spectra of a typical Ru(II)−polypyridine complex.

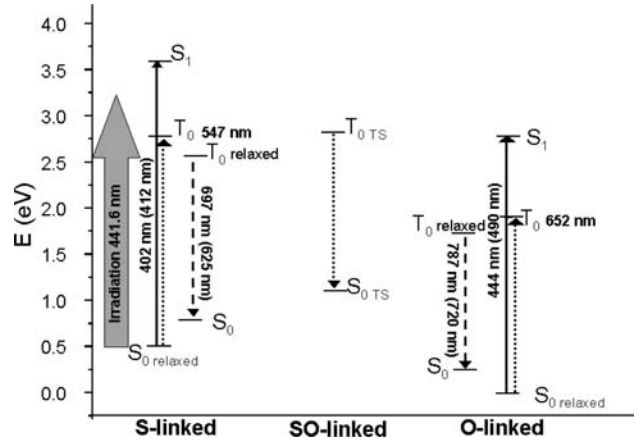

FIGURE 4. Schematic representation of the computed (TD-DFT) relative energy of the ground (S_0) and first singlet (S_1), and first triplet (T_1) excited states of several conformers of $[Ru(bpy)(tpy)dmso]^{2+}$ and computed absorption/emission energies. Full line arrows correspond to computed allowed transitions, dotted arrows to nonallowed ones, and dashed arrows to the computed emission. Experimental values are reported in parenthesis; *relaxed* stands for computed at the corresponding optimized structure, and TS indicates a transition state.

many other dyes,[25] we can conclude that our computational protocol is reliable for quantitative color estimates of organic derivatives.

3.2. Absorption of Inorganic Dyes. There are few systematic studies dealing with the effect of the computational protocol on the modeling of given excited states in inorganic dyes. This is mainly due to their size (in terms of atom numbers and active electrons) and, contrary to organic dyes, to the difficulty to obtain large sets of similar compounds. Focusing on inorganic dyes including d transition metal atoms, the TD-DFT approach, in conjunction with the PBE0 functional, well reproduces the metal to ligand charge transfer bands (MLCT) usually responsible for their strong absorption in the visible region. Illustrative examples are the complexes of the Ru−polypyridine family for which the experimental transitions and the band shape are both nicely reproduced (see Figures 3 and 4).[26−32] However, the errors are larger than for organic molecules, ranging between 0.15 and 0.40 eV. Furthermore, it is a matter of fact that for such complex systems, associated experimental facts are seldom straightforwardly rationalized. In this context, theoretical methods again constitute a valuable means to interpret and even anticipate photochemical behaviors.[26,30,32,33] A clear example is the phototriggered isomerization (PTI) process undergone by the $[Ru(bpy)(tpy)dmso]^{2+}$ complex (bpy = 2,2′-bipyridine; dmso = dimethyl sulfoxide) for which theory has amended and anticipated the experimental evidence of the pathway of photoisomerization. In this system, the sixth position on the octahedral coordination sphere of Ru(II) is constituted by dmso that can either bind to the sulfur atom (S-linked isomer) or to the oxygen (O-linked isomer).

The S-linked isomer of $[Ru(bpy)(tpy)dmso](CF_3SO_3)_2$ undergoes an immediate color change upon irradiation at 441.6 nm: the absorption is shifted from 412 to 490 nm, and the corresponding photoproduct is stable for days. Upon excitation, the complex also displays a weak luminescence (λ_{em} = 720 nm) at room temperature, while a new additional emission feature appears at 625 nm upon cooling to 170 K.[34] These observations lead to the proposal of a rather complicated reaction path, where the isomerization mechanism takes place in the lowest triplet or singlet excited states and involves a hypothetical η_2 species, characterized by concomitant S- and O- linkages to the metal cation. This η_2 structure was supposed to be responsible for the weak emission at 625 nm.[34] The theoretical reaction pathway clearly appears different.[35] Indeed, while the $S_0 \rightarrow S_1$ absorption of both S- and O-linked species, as well as the emission from the O-linked triplet state, are correctly reproduced, no evidence of the formation of the a stable η_2 species can be found. Both in the ground and in triplet excited states, η_2 truly corresponds to a transition state (TS), see Figure 4. Furthermore, the emission at 625 nm could be attributed to the decay of the triplet state of the S-bonded isomer computed at 697 nm.

This apparent discrepancy was finally conciliated when new experimental data[36] confirmed the validity of the theoretical outcomes, pointing out that the reaction actually proceeds within a direct one-step mechanism, and as predicted by theory, the SO-linked η_2 species is the TS. This example, though based on a quite simple light triggered phenomenon, clearly illustrates the essential role that computational approaches can play in the interpretation of complex photoinduced phenomena.

3.3. Fluorescence. The theoretical framework allowing for the computation of geometric gradients at the TD-DFT level[8]

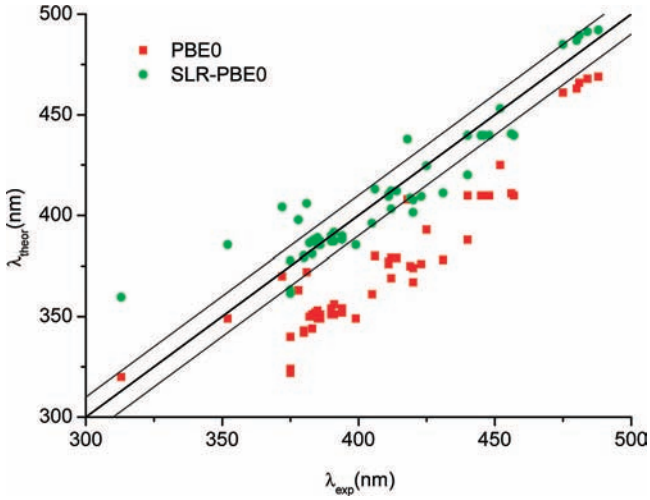

FIGURE 5. Comparison between theoretical and experimental λ_{max}^{fluo} of substituted coumarins. The central line indicates a perfect theory/experiment match, whereas the two side lines are boundaries for ±10 nm deviation.

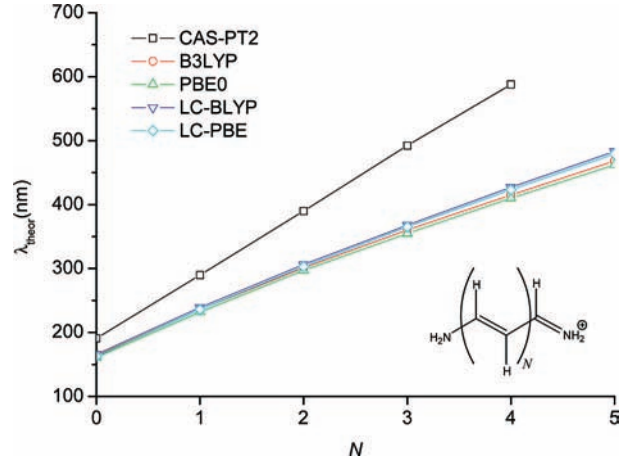

FIGURE 6. Absorption maxima (nm) of the first dipole-allowed electronic transition as a function of the chain length (*N*) in model cyanines.

has paved the way toward the calculation of the excited-state structures of large molecules, hence, the determination of fluorescence. Nevertheless, solvent effects in a PCM framework were only recently included in a TD-DFT approach.[9] Consequently, the number of works assessing the efficiency of TD-DFT for the calculation of fluorescence wavelengths of a statistically significant set of dyes is still limited, because the largest investigations were performed for neutral and charged coumarins (Figure 1),[37,38] for which PCM-TD-DFT correctly reproduces the modifications induced by auxochromic effects for the emission properties. Indeed, a simple linear regression applied to PCM-TD-DFT results allows one to obtain a perfect match with measurements whatever the form of the coumarin dye (enol, keto, cation, or anion). This approach returns absolute estimates with very small average errors (0.07 eV, Figure 5). More importantly, the absorption−fluorescence Stokes shift for a given compound is only slightly underestimated. Furthermore, the direct TD-DFT optimization of the excited-state structure allows one to avoid the use of CIS structures to estimate fluorescence wavelengths. This circumvents a problematic approximation as electron-correlation effects differ for the ground and excited state. In addition, the symmetry of the excited-state geometries and the solvatochromic effects appears to be not always consistently reproduced by CIS.[38]

In order to test the performance of TD-DFT for the description of the fluorescence properties of inorganic dye, the spectral properties of an Al(III) complex of 8-hydroxyquinoline-5-sulfonic acid (Al(III)(8-HQS)$_3$) were computed.[39] This latter was considered due to its strong fluorescence both in solution and in solid state, making it a reference compound for application as emissive material in the emerging display technology based on organic light-emitting diodes (OLEDs).[40] Ligand-centered $\pi-\pi^*$ transitions of HOMO−LUMO type are responsible for the absorption of the complex in the near-UV. Its fluorescence ($S_1 \rightarrow S_0$), observed between 475 and 485 nm,[41] is computed at 488 nm, in excellent agreement with the experimental data. Indeed, calculations not only nicely reproduce the measured bands and Stoke shift but also give access to the geometrical structure of the excited state. In particular, the analysis of the geometrical parameters corresponding to the optimized S_1 structure validates the experimental assumption that within the complex the Al cation plays the same role as a proton for the isolated ligand, the structural change in the complex being similar to those obtained for the photoinduced tautomerization observed for the isolated ligand.

4. Breakdowns and Perspectives

The computational protocols above-described can generally be applied to the calculation of optical properties of dyes. However, it is clear that when dealing with TD-DFT approaches, the recognized failures of DFT for the ground state due to the use of approximate functionals (such as the lack of nondynamical electronic correlation or the self-interaction error) sum up to others specific to the excited states model (LDA kernel, missing of double excitations, response treatment limited to linear term, lack of the $1/r$ asymptotical behavior). From a practical point of view, the two most problematic cases are represented by systems characterized by multireference electronic states or when dealing with transitions of charge transfer (CT) type.

An example of the former breakdown can be illustrated by the cyanine derivatives (Figure 6), for which standard DFT

TABLE 1. Statistical Analysis for 9,10-Anthraquinone (AQ), Azobenzene (AB), and Indigoid (IG) Dye Series[a]

		without fit				with linear correction	
family	method	MSE	MAE	rms	R^2	MAE	rms
AQ	HF	127	127	132	0.97	11	14
	PBE	−71	74	80	0.78	28	36
	PBE0	12	19	27	0.96	12	15
	LC-PBE[b]	67	67	71	0.98	8	10
	LC-ωPBE[b]	85	85	89	0.99	8	9
	CAM-B3LYP	53	33	58	0.98	8	10
AB	HF	64	64	75	0.89	15	21
	PBE	−90	90	103	0.83	22	27
	PBE0	−20	25	27	0.93	12	17
	LC-PBE	33	33	43	0.95	10	14
	LC-ωPBE	46	46	54	0.96	10	14
	CAM-B3LYP	15	20	28	0.94	10	16
IG	HF	170	170	174	0.89	19	26
	PBE	−96	96	116	0.71	34	42
	PBE0	6	19	23	0.93	17	21
	LC-PBE	70	70	72	0.97	10	13
	LC-ωPBE	99	99	101	0.97	12	14
	CAM-B3LYP	58	58	60	0.98	10	12
all	HF	116	116	127	0.76	37	45
	PBE	−86	87	102	0.81	30	40
	PBE0	−3	22	29	0.91	22	28
	LC-PBE	52	52	58	0.94	18	23
	LC-ωPBE	71	71	78	0.94	18	23
	CAM-B3LYP	37	38	46	0 0.93	20	25

[a] All data are in nanometers and are from ref 25. [b] Please note that LC-PBE and LC-ωPBE differ both in how the short-range contribution is derived and in the range separation parameter, ω (0.33 b^{-1} in LC-PBE and 0.40 b^{-1} in LC-ωPBE).[44]

approaches fail in predicting the evolution of λ_{max} with increasing chain length.[42]

The CT problem was nicely underlined in model systems, where the electron donor and acceptor are fully electronically decoupled.[43] In such conditions (zero overlap between the two moieties), both GGA and GH approaches significantly underestimate the electronic transition energies. This is no longer the case for RSH methods, such as LC-ωPBE[44] or CAM-B3LYP,[45] for which the variation (but not always the absolute value) of the CT bands with respect to the donor−acceptor distance can be adequately reproduced.[46] However, if the two parts have an even minimal orbital overlap, CT transitions can correctly be reproduced even using standard GH, as demonstrated by several studies on coordination chemistry compounds[26,30,33] and on typical organic dyes.[47] More generally, RSH models represent a further step toward a greater accuracy,[48] even if the improvement with respect to the PBE0 results is not systematic, as nicely summarized in the data of Table 1, where the λ_{max} of several families of organic dyes are reported.[25]

Finally, it is worth mentioning that if a calculation protocol for vertical transition energies in organic dyes can be well defined, still in order to get a realistic simulation of absorption spectra (band shape and observed transition energies) of even very simple systems, another ingredient is still missing: the calculation of vibronic effects. Recent advances in the calculation of Franck−Condon factors, also feasible for relatively medium-sized compounds, pave the way toward even more realistic computation of dye spectra.[49,50]

The authors are grateful to the numerous researchers that have contributed (in alphabetical order): J-M. André, X. Assfeld, M. Bouhy, L. Briquet, M. Charlot, C. A. Daul, M. J. Frisch, M. Fontaine, R. Kobayashi, P. P. Lainé, C. Lambert, A. L. Laurent, T. Le Bahers, P.-F. Loos, F. Maurel, C. Peltier, J. Preat, G. Scalmani, G. E. Scuseria, D. P. Vercauteren, O. A. Vydrov, and V. Wathelet. We are indeed convinced that any long-term scientific collaboration is based on successful human relationships. D.J. and E.A.P. thank the Belgian National Fund for their research associate positions. The authors thank the Commissariat Général aux Relations Internationale and the Egide agency for supporting this work within the framework of the Tournesol Scientific cooperation between France and the Communauté Française de Belgique. C.A. and I.C. are grateful to the French National Agency for Research (ANR) (NEXUS project; No BLAN07-1_196405) for financial support. Several calculations have been performed on the Interuniversity Scientific Computing Facility (ISCF), installed at the FUNDP (Namur, Belgium), for which the authors gratefully acknowledge the financial support of the FNRS-FRFC and the "Loterie Nationale" for the convention number 2.4578.02, and of the FUNDP.

BIOGRAPHICAL INFORMATION

Denis Jacquemin was born in Dinant (Belgium) in 1974; he received his Ph.D. in Chemistry from the University of Namur in 1998. He then went to University of Florida for his postdoctoral stay. Since 2003, he has been Research Associate of the FNRS. His research interests are the investigation of the spectroscopic properties of conjugated molecules and polymers.

Eric A. Perpète was born in Dinant (Belgium) in 1970. He received his Ph.D. in Chemistry at the University of Namur in 1997, and then he moved to University of California for a postdoctoral stay. Since 1998, he has been research associate of the FNRS, and he was visiting researcher at the University of Girona (Spain) and Université Henri Poincaré (France). His research interests are related to molecular spectroscopic properties, including electronic spectra and nonlinear optics properties.

Ilaria Ciofini was born in Arezzo (Italy) in 1973. After a degree in Chemistry at the University of Florence (Italy), she moved to Switzerland to get a Ph.D. in Theoretical Chemistry from the University of Fribourg in 2001. After, she spent one year as a postdoctoral fellow at the University of Würzburg (Germany), followed by two years as associate CNRS researcher at the ENSCP in Paris (France). Since 2004, she has been IR-CNRS at the ENSCP. Her

main research interests are related to the investigation of magnetic and spectroscopic properties of coordination compounds.

Carlo Adamo was born in Naples (Italy) in 1963, where he did all his studies at University Federico II, receiving a Ph.D. in Theoretical Chemistry in 1995. Between 1993 and 2000, he was Assistant Professor at the University of Basilicata (Italy). In 2000, he moved to ENSCP (France) as Associate Professor where he became Full Professor in Theoretical Chemistry in 2004. He was visiting researcher at CEA-Grenoble (France), Rice University (USA), University Joseph Fourier (France), and University Federico II (Italy). His main research interests concern development of new DFT approaches and their applications to various fields of chemistry.

FOOTNOTES

* Corresponding authors. E-mail addresses: denis.jacquemin@fundp.ac.be; carlo-adamo@enscp.fr

REFERENCES

1 Christie, R. M. *Colour Chemistry*; The Royal Society of Chemistry: Cambridge, U.K., 1971.

2 Lehn, J. M. Perspectives in supramolecular chemistry - from molecular recognition towards molecular information processing and self-organization. *Angew. Chem., Int. Ed.* **1990**, *29*, 1304–1319.

3 Juris, A.; Balzani, V.; Barigelletti, F.; Belser, P.; Von Zelewsky, A. Ru(II) polypyridine complexes: Photophysics, photochemistry, eletrochemistry, and chemiluminescence. *Coord. Chem. Rev.* **1988**, *84*, 85–277.

4 See for instance Balzani, V.; Juris, A.; Venturi, M.; Campagna, S.; Serroni, S. Luminescent and redox-active polynuclear transition metal complexes. *Chem. Rev.* **1996**, *96*, 759–833.

5 Koch, W.; Holthausen, M. C. A. *Chemist's Guide to Density Functional Theory*; Wiley-VCH: New York, 2000.

6 Runge, E.; Gross, E. K. U. Density-functional theory for time-dependent systems. *Phys. Rev. Lett.* **1984**, *52*, 997–1000.

7 van Caillie, C.; Amos, R. D. Geometric derivatives of excitation energies using SCF and DFT. *Chem. Phys. Lett.* **1999**, *308*, 249–255.

8 Scalmani, G.; Frisch, M. J.; Mennucci, B.; Tomasi, J.; Cammi, R.; Barone, V. Geometries and properties of excited states in the gas phase and in solution: Theory and application of a time-dependent density functional theory polarizable continuum model. *J. Chem. Phys.* **2006**, *124*, 094107.

9 Becke, A. D. Density-functional thermochemistry. 3. The role of exact exchange. *J. Chem. Phys.* **1993**, *98*, 5648–5652.

10 Jaramillo, J.; Scuseria, G. E.; Ernzerhof, M. Local hybrid functionals. *J. Chem. Phys.* **2003**, *118*, 1068–1073.

11 Iikura, H.; Tsuneda, T.; Yanai, T.; Hirao, K. A long-range correction scheme for generalized-gradient-approximation exchange functionals. *J. Chem. Phys.* **2001**, *115*, 3540–3544.

12 Adamo, C.; Barone, V. Toward reliable density functional methods without adjustable parameters: The PBE0 model. *J. Chem. Phys.* **1999**, *110*, 6158–6170. Ernzerhof, M.; Scuseria, G. E. Assessment of the Perdew—Burke—Ernzerhof exchange-correlation functional. *J. Chem. Phys.* **1999**, *110*, 5029. Such a functional is also known with the acronym PBE1PBE (the keyword in the Gaussian program) or PBEh..

13 Adamo, C.; Scuseria, G. E.; Barone, V. Accurate excitation energies from time-dependent density functional theory, assessing the PBE0 model. *J. Chem. Phys.* **1999**, *111*, 2889–2899.

14 Ciofini, I.; Adamo, C. Accurate evaluation of valence and low-lying rydberg states with standard time-dependent density functional theory. *J. Phys. Chem. A* **2007**, *111*, 5549–5556.

15 Tomasi, J.; Mennucci, B.; Cammi, R. Quantum mechanical continuum solvation models. *Chem. Rev.* **2005**, *105*, 2999–3093.

16 Cossi, M.; Barone, V. Time-dependent density functional theory for molecules in liquid solutions. *J. Chem. Phys.* **2001**, *115*, 4708–4717.

17 Jacquemin, D.; Preat, J.; Charlot, M.; Wathelet, V.; André, J. M.; Perpète, E. A. Theoretical investigation of substituted anthraquinone dyes. *J. Chem. Phys.* **2004**, *121*, 1736–1743.

18 Perpète, E. A.; Wathelet, V.; Preat, J.; Lambert, C.; Jacquemin, D. Toward a theoretical quantitative estimation of the λ_{max} of anthraquinones-based dyes. *J. Chem. Theory. Comput.* **2006**, *2*, 434–440.

19 Jacquemin, D.; Wathelet, V.; Preat, J.; Perpète, E. A. Ab initio tools for the accurate prediction of the visible spectra of anthraquinones. *Spectrochim. Acta A* **2007**, *67*, 334–341.

20 Preat, J.; Jacquemin, D.; Perpète, E. A. A TD-DFT investigation of the visible spectra of fluoro-anthraquinones. *Dyes Pigm.* **2007**, *72*, 185–191.

21 Jacquemin, D.; Preat, J.; Assfeld, X.; Perpète, E. A. Comparison of theoretical approaches for predicting the UV/vis spectra of anthraquinones. *Mol. Phys.* **2007**, *105*, 325–331.

22 Jacquemin, D.; Preat, J.; Wathelet, V.; Fontaine, M.; Perpète, E. A. Thioindigo dyes: Highly accurate visible spectra with TD-DFT. *J. Am. Chem. Soc.* **2006**, *128*, 2072–2083.

23 Jacquemin, D.; Preat, J.; Wathelet, V.; Perpète, E. A. Substitution and chemical environment effects on the absorption spectrum of indigo. *J. Chem. Phys.* **2006**, *124*, 074104.

24 Perpète, E. A.; Preat, J.; André, J. M.; Jacquemin, D. An ab initio study of the absorption spectra of indirubin, isoindigo and related compounds. *J. Phys. Chem. A* **2006**, *110*, 5629–5635.

25 Jacquemin, D.; Perpète, E. A.; Scuseria, G. E.; Ciofini, I.; Adamo, C. TD-DFT performance for the visible absorption spectra of organic dyes: Conventional versus long-range hybrids. *J. Chem. Theory Comput.* **2008**, *4*, 123–135.

26 Ciofini, I.; Lainé, P. P.; Bedioui, F.; Adamo, C. Photoinduced intramolecular electron transfer in ruthenium and osmium polyads: Insights from theory. *J. Am. Chem. Soc.* **2004**, *126*, 10763–10777.

27 Lainé, P. P.; Ciofini, I.; Ochsenbein, P.; Amouyal, E.; Adamo, C.; Bedioui, F. Photoinduced processes within compact dyads based on triphenylpyridinium-functionalised bypiridil complexes of ruthenium(II). *Chem.—Eur. J.* **2005**, *11*, 3711–3727.

28 Ciofini, I.; Lainé, P. P.; Bedioui, F.; Daul, C. A.; Adamo, C. Theoretical modelling of photochemical molecular devices: insights using Density Functional Theory. *C. R. Chim.* **2006**, *9*, 226–239.

29 Ciofini, I. Exploring the photophysical behaviour of supramolecular systems: Problems and perspectives. *Theor. Chem. Acc.* **2006**, *116*, 219–231.

30 Lainé, P. P.; Loiseau, F.; Campagna, S.; Ciofini, I.; Adamo, C. Conformationally gated photoinduced processes within photosensitizer - acceptor dyads based on osmium(II) complexes with triarylpyridinio-functionalized terpyridyl ligands. 2. Insights from theoretical analysis. *Inorg. Chem.* **2006**, *45*, 5538–5551.

31 Labat, F.; Lainé, P. P.; Ciofini, I.; Adamo, C. Spectral properties of bipyridyl ligands by Time Dependent Density Functional Theory. *Chem. Phys. Lett.* **2006**, *417*, 445–451.

32 Rekhis, M.; Labat, F.; Ouamerali, O.; Ciofini, I.; Adamo, C. A theoretical analysis of the electronic properties of N3 derivatives. *J. Phys. Chem. A* **2007**, *111*, 13106–13111.

33 Guillemoles, J.-F.; Barone, V.; Joubert, L.; Adamo, C. A theoretical investigation of the ground and excited states of selected Ru and Os polypyridyl molecular dyes. *J. Phys. Chem. A* **2002**, *106*, 11354–11360.

34 Rack, J. J.; Winkler, J. R.; Gray, J. B. Phototriggered Ru(II)-dimethylsulfoxide linkage isomerization in crystals and films. *J. Am. Chem. Soc.* **2001**, *123*, 2432–2433.

35 Ciofini, I.; Daul, C. A.; Adamo, C. Photo-triggered linkage isomerization of ruthenium—dimethylsulfoxide: Insights from theory. *J. Phys. Chem. A* **2003**, *107*, 11182–11190.

36 Rachford, A. A.; Rack, J. J. Picosecond isomerization in photochromic ruthenium—dimethyl sulfoxide complexes. *J. Am. Chem. Soc.* **2006**, *128*, 14318–14324.

37 Jacquemin, D.; Perpète, E. A.; Scalmani, G.; Frisch, M. J.; Assfeld, X.; Ciofini, I.; Adamo, C. TD-DFT investigation of the absoprtion, fluorescence and phosphorescence spectra of solvated coumarins. *J. Chem. Phys.* **2006**, *125*, 164324.

38 Jacquemin, D.; Perpète, E. A.; Assfeld, X.; Scalmani, G.; Frisch, M. J.; Assfeld, X.; Adamo, C. The geometries, absorption and fluorescence wavelengths of solvated fluorescent coumarins: A CIS and TD-DFT comparative study. *Chem. Phys. Lett.* **2007**, *438*, 208–212.

39 Le Bahers, T.; Adamo, C.; Ciofini, I. Manuscript in preparation.

40 See, for instance: Tang, C. W.; VanSlykev, S. A. Organic electroluminescent diodes. *Appl. Phys. Lett.* **1987**, *51*, 913–915. Hopkins, T. A.; Meerholz, K.; Shadeen, S.; Anderson, M. L.; Schimdt, A.; Kippelen, B.; Padias, A. B.; Hall, H. K.; Peyghambarian, N., Jr.; Armstrong, N. R. Substituted aluminium and zinc quinolate with blue-shifted absorbance/luminescence bands: synthesis and spectroscopic, photoluminescence and electroluminescence characterization. *Chem. Mater.* **1996**, *8*, 344–351.

41 (a) Mulon, J. B.; Destandau, E.; Alain, V.; Bardez, E. How can aluminium(III) generate fluorescence? *J. Inorg. Biochem.* **2005**, *99*, 1749–1755. (b) Muegge, B. D.; Brooks,

S.; Richter, M. M. Richter, M. M. Electrochemiluminescence of tris(8-hydroxyquinoline-5-sulfonic acid)aluminium(III) in aqueous solution. *Anal. Chem.* **2003**, *75*, 1102–1105.

42 Jacquemin, D.; Perpète, E. A.; Scalmani, G.; Frisch, M. J.; Kobayashi, R.; Adamo, C. An assessment of the efficiency of long-range corrected functionals for some properties of large compounds. *J. Chem. Phys.* **2007**, *126*, 144105.

43 Dreuw, A.; Weisman, J. L.; Head-Gordon, M. Long-range charge-transfer excited states in time-dependent density functional theory require non-local exchange. *J. Chem. Phys.* **2003**, *119*, 2943–2946.

44 Vydrov, O. A.; Scuseria, G. E. Assessment of a long-range corrected hybrid functional. *J. Chem. Phys.* **2005**, *125*, 234109.

45 Yanai, T.; Tew, D. P.; Handy, N. C. A new hybrid exchange-correlation functional using the Coulomb-attenuating method (CAM-B3LYP). *Chem. Phys. Lett.* **2004**, *393*, 51–57.

46 Peach, M. J. G.; Benfield, P.; Helgaker, T.; Tozer, D. J. Excitation energies in density functional theory: An evaluation and a diagnostic test. *J. Chem. Phys.* **2008**, *128*, 044118.

47 Jacquemin, D.; Bouhy, M.; Perpète, E. A. Excitation spectra of nitro-diphenylaniline: Accurate time-dependent density functional theory predictions for charge-transfer dyes. *J. Chem. Phys.* **2006**, *124*, 204321.

48 Jacquemin, D.; Perpète, E. A.; Vydrov, O. A.; Scuseria, G. E.; Adamo, C. Assessment of long-range corrected functionals performance for n$-\pi^*$ transitions in organic dyes. *J. Chem. Phys.* **2007**, *127*, 094102.

49 Dierksen, M.; Grimme, S. A density functional calculations of the vibronic structure of electronic absorption spectra. *J. Chem. Phys.* **2004**, *120*, 3544–3554.

50 Improta, R.; Barone, V.; Santoro, F. Ab Initio calculations of absorption spectra of large molecules in solution: Coumarin C15. *Angew. Chem., Int. Ed.* **2007**, *46*, 405–408.